Memorias del 2023 Congreso Nacional de Control Automático
25-27 de Octubre, 2023. Acapulco, Guerrero, México.

Comparison of Formation Algorithms with Collision Avoidance for Second-order Agents ⋆

Juan Francisco Flores-Resendiz * **Jaime González-Sierra** **
Eduardo Aranda-Bricaire ***

* *Faculty of Engineering, Administrative and Social Sciences, Autonomous University of Baja California, Tecate 21460, Mexico (e-mail: francisco.flores32@uabc.edu.mx)*
** *Unidad Profesional Interdisciplinaria de Ingeniería Campus Hidalgo, Instituto Politécnico Nacional, San Agustín Tlaxiaca 42162, Hidalgo, Mexico (e-mail: jagonzalezsi@ipn.mx)*
*** *Mechatronics Section, Department of Electrical Engineering, CINVESTAV, Mexico City 07360, Mexico (e-mail: earanda@cinvestav.mx)*

Abstract: This work compares two novel strategies that address formation control with collision avoidance for a group of second-order agents. The first control strategy is based on the Backstepping approach (B), while the second is based on the Nested Saturation methodology (NS). Both approaches utilize the Repulsive Vector Fields (RVFs) approach for avoiding collisions. Two numerical simulations are carried out to compare the performance of both approaches. For the first numerical simulation, the simplest case of collision avoidance is considered, that is, the interchange of the position of two agents. On the other hand, for the second numerical simulation, the formation with collision avoidance for a group of nine agents is considered.

Keywords: Multi-agent system, Second-order agents, Formation control, Collision avoidance.

1. INTRODUCTION

Multi-agent systems have a broad avenue for specific research areas (Draganjac et al., 2016; Guanghua et al., 2013; Madridano et al., 2021; Yan and Ma, 2019). From the Automatic Control and Robotics point of view, one of the simplest ways to picture the problem is to imagine a set of n agents wandering in some space. It is natural to imagine that the user wants them to move towards a specific goal. It is also natural to desire that, in their motion, the agents do not collide amongst themselves. This is a very rough manner of introducing the problem under study in the current paper.

This problem has been thoroughly treated over the years by many authors. Perhaps the seminal contribution is the one reported in (Khatib, 1985). However, several difficulties of Khatib's approach were put forward in a series of papers (Flores-Resendiz et al., 2015; Flores-Resendiz and Aranda-Bricaire, 2020; Hernández-Martínez and Aranda-Bricaire, 2011; Hernandez-Martinez and Aranda-Bricaire, 2013). In those papers, the problem of first-order agents was wholly solved using the novel technique of repulsive (not necessarily) integrable vector fields.

The passing from first-form first-order systems to second-order ones is not trivial. For a straightforward reason: second-order systems possess inertia. Therefore, even if the control algorithm foresees a collision, sometimes it is impossible to avoid such an event. This is the subject matter of this paper. Some examples of collision avoidance for second-order agents are reported in (Dang et al., 2019; Huang et al., 2019; Liu et al., 2022; Park and Yoo, 2021; Parra-Marín et al., 2023; Yasin et al., 2020), where different methodologies, approaches, and algorithms were proposed.

The authors have proposed some algorithms that prevent possible collisions and act in advance to avoid such an event. We compare a couple of strategies, both relying on the aforementioned repulsive vector fields. Both algorithms are compared through numeral simulations and a performance index.

⋆ Jaime González-Sierra gratefully acknowledges the financial support from Instituto Politécnico Nacional by Project SIP: 20230121.

2. PRELIMINARIES

Consider $N = \{R_1, \ldots, R_n\}$ as a set of n agents with second-order dynamics

$$\dot{\mathbf{z}}_i = \mathbf{v}_i, \quad \dot{\mathbf{v}}_i = \mathbf{u}_i, \quad i = 1, \ldots, n,$$

where $\mathbf{z}_i = [x_i \ y_i]^\top \in \mathbb{R}^2$ is the position in the plane of the i-th agent while $\mathbf{v}_i = [v_{x_i} \ v_{y_i}]^\top \in \mathbb{R}^2$ and $\mathbf{u}_i = [u_{x_i} \ u_{y_i}]^\top \in \mathbb{R}^2$ represent the velocities and accelerations along the X and Y axis, respectively. In matrix form, one has

$$\dot{\mathbf{z}} = \mathbf{v}, \quad \dot{\mathbf{v}} = \mathbf{u}, \tag{1}$$

where $\mathbf{z} = \begin{bmatrix}\mathbf{z}_1^\top & \ldots & \mathbf{z}_n^\top\end{bmatrix}^\top \in \mathbb{R}^{2n}$ and $\mathbf{u} = \begin{bmatrix}\mathbf{u}_1^\top & \ldots & \mathbf{u}_n^\top\end{bmatrix}^\top \in \mathbb{R}^{2n}$.

Definition 1. (Formation graph). A formation graph $\mathcal{G}$ (Godsil and Royle (2001); Ren and Beard (2008)), relates the communication among the agents and it is composed by three elements:

(1) A set of vertices N. Each vertex simulates an agent in the system.
(2) A set of edges $E = \{(R_j, R_i) \in N \times N, j \neq i\}$. In this case, agent R_i receives information from R_j.
(3) A set of labels $C = \{\mathbf{c}_{ji} \in \mathbb{R}^2 \mid (R_j, R_i) \in N \times N, j \neq i\}$, where $\mathbf{c}_{ji} = \begin{bmatrix}c_{ji_x} & c_{ji_y}\end{bmatrix}^\top \in \mathbb{R}^2$ is a vector that specifies the relative position between agents R_j and R_i.

Definition 2. (Laplacian matrix). Given a formation graph $\mathcal{G}$, the Laplacian matrix of $\mathcal{G}$ (Godsil and Royle, 2001; Ren and Beard, 2008) is defined as $\mathcal{L}(\mathcal{G}) = \Delta - \mathcal{A}_d$ where $\Delta = \text{diag}\{n_1, \ldots, n_n\}$ is the degree matrix with $n_i = \text{card}\{N_i\}$, and $N_i \subset N$ is a subset composed by those agents that are detected by R_i. Matrix $\mathcal{A}_d$ is the adjacency matrix of $\mathcal{G}$ given by

$$a_{ij} = \begin{cases} 1 & \text{if} \quad (R_j, R_i) \in E, \\ 0 & \text{otherwise.} \end{cases}$$

The desired position of each agent, in a formation graph $\mathcal{G}$, is defined as

$$\mathbf{z}_i^* = \frac{1}{n_i} \sum_{j \in N_i} (\mathbf{z}_j + \mathbf{c}_{ji}), \quad i = 1, \ldots, n. \tag{2}$$

Furthermore, let us define the position error as $\tilde{\mathbf{z}}_i = \mathbf{z}_i - \mathbf{z}_i^*$; hence, in matrix form, one has

$$\tilde{\mathbf{z}} = \left(\Delta^{-1}\mathcal{L} \otimes I_2\right)\mathbf{z} - \left(\Delta^{-1} \otimes I_2\right)\mathbf{c}, \tag{3}$$

where $\otimes$ denotes the Kronecker product, and I_2 is the identity matrix, while

$$\mathbf{c} = \begin{bmatrix} \sum_{j \in N_1} \mathbf{c}_{j1} \\ \vdots \\ \sum_{j \in N_n} \mathbf{c}_{jn} \end{bmatrix} \tag{4}$$

is a vector that contains the formation vectors.

Definition 3. (Linear saturation (Teel, 1992)). Given two positive constants M_1, M_2 with $M_1 \leq M_2$, a function $\sigma : \mathbb{R} \to \mathbb{R}$ is said to be a linear saturation for (M_1, M_2) if it is a continuous, non-decreasing function satisfying the following:

(1) $x\sigma(x) > 0$, for all $x \neq 0$;
(2) $\sigma(x) = x$ when $|x| \leq M_1$;
(3) $|\sigma(x)| \leq M_2$, for all $x \in \mathbb{R}$.

Definition 4. Let Φ_r be the set of the saturating functions which is composed of all the real functions which satisfy the following conditions

(1) $\phi(x) = 0 \Leftrightarrow x = 0$;
(2) $-r \leq \phi(x) \leq r$ for some $r > 0$;
(3) $x\phi(x) > 0$, $\forall x \neq 0$;
(4) $0 < \frac{\partial \phi(x)}{\partial x} < \bar{M}_1 < \infty$.

Then, it is said $\phi_r(\cdot)$ is a saturating function parameterized by r.

2.1 Repulsive Vector Fields

The collision avoidance algorithm is based on the RVFs approach. This technique considers that there exists an unstable focus centered on the position of any other agent or obstacle. The main idea is to activate the RVFs when agents are near enough to each other and deactivate them when they are far enough. Concretely, the RVF is defined as

$$\boldsymbol{\beta}_i = -\epsilon \sum_{j \in \mathcal{M}_i} \psi_{ij}(d_{ij}) \begin{bmatrix}(x_j - x_i) - (y_j - y_i) \\ (x_j - x_i) + (y_j - y_i)\end{bmatrix}, \tag{5}$$

where $\epsilon > 0$ scales the RVF; $\mathcal{M}_i$ is a set composed of all those agents that are at risk of collision with agent R_i, *i.e.*,

$$\mathcal{M}_i = \{R_j \in N \mid \|\mathbf{z}_i - \mathbf{z}_j\| \leq D\}, \quad i = 1, .., n,$$

D is the sensing distance; $\psi_{ij}(\cdot)$ is a smooth distance-based switching function which satisfies $\psi_{ij}(d_{ij}) = 1$ for $d_{ij} < d$ and $\psi_{ij}(d_{ij}) = 0$ for $d_{ij} > D$; and $d_{ij} = \|\mathbf{z}_i - \mathbf{z}_j\|$ is the distance between R_i and R_j.

3. CONTROL ALGORITHMS

This Section presents two control strategies that solve the formation control with collision avoidance for a group of second-order agents. The former is based on the Backstepping approach (B), while the second one is based on the nested saturation methodology (NS). It is said that there are no collisions among agents if the agents remain at some minimum predefined distance d from each other, that is, $\|z_i(t) - z_j(t)\| \geq d$, $\forall t \geq 0$, $i \neq j$.

3.1 Backstepping approach with RVFs

This control law was developed starting from a solution to the collision avoidance problem regarding first-order agents. Then, an additional backstepping stage was designed to apply the control strategy to second-order agents. Input-to-state property is utilized to prove convergence to agents to the desired formation while they

keep a minimum distance among them. This result was previously reported in (Flores-Resendiz et al., 2023).

Under this approach, the proposed control law is

$$\mathbf{u} = -\lambda\mu\phi(\tilde{\mathbf{z}}) + \epsilon\left(\left(\lambda\Omega + \dot{\Omega}\right)\otimes F\right)\mathbf{z} - \left(\mu\left(\frac{\partial\phi(\tilde{\mathbf{z}})}{\partial\tilde{\mathbf{z}}}\right)^{T}\left(\Delta^{-1}\mathcal{L}(G)\otimes I_2\right) + \lambda I_{2n} - \epsilon\left(\Omega\otimes F\right)\right)\mathbf{v}, \tag{6}$$

where the matrix Ω, which depends on the distance between every pair of agents and models the conflicts among agents, is described by

$$\Omega = \begin{bmatrix} \sum_{j=1,j\neq i}^{n}\psi(d_{1j}) & \dots & -\psi(d_{in}) \\ \vdots & \ddots & \vdots \\ -\psi(d_{n1}) & \dots & \sum_{j=1,j\neq i}^{n}\psi(d_{nj}) \end{bmatrix}. \tag{7}$$

As it can be seen, because of the design process, the RVFs are embedded into the control law. Furthermore,

$$F = \begin{bmatrix} 1 & -1 \\ 1 & 1 \end{bmatrix}, \tag{8}$$

is the matrix which provides the unstable focus behaviour and

$$\left(\frac{\partial\phi(\tilde{\mathbf{z}})}{\partial\tilde{\mathbf{z}}}\right)^{T} = \operatorname{diag}\left\{\left(\frac{\partial\phi(\tilde{\mathbf{z}}_1)}{\partial\tilde{\mathbf{z}}_1}\right)^{T},\dots,\left(\frac{\partial\phi(\tilde{\mathbf{z}}_n)}{\partial\tilde{\mathbf{z}}_n}\right)^{T}\right\}. \tag{9}$$

Finally, μ, λ and ϵ are positive constants; $\phi(\cdot)$ is a saturation function (Definition 4) and I_{2n} is the identity matrix of dimension $2n$.

3.2 Nested saturation approach with RVFs

This control law was designed employing the nested saturation approach (developed by (Teel, 1992)) to accomplish formation control while RVFs are added to avoid collisions among the agents. Based on those mentioned above and in the work of (Aranda-Bricaire and González-Sierra, 2023), the control law is given by

$$\mathbf{u} = -\boldsymbol{\sigma}_2\left(\eta\left(\Delta^{-1}\mathcal{L}\otimes I_2\right)\mathbf{v} + \boldsymbol{\sigma}_1(\eta\tilde{\mathbf{z}} + \mathbf{v})\right) + \boldsymbol{\beta}, \tag{10}$$

where $\boldsymbol{\beta} = \left[\boldsymbol{\beta}_1^{\top}\ \dots\ \boldsymbol{\beta}_n^{\top}\right]^{\top} \in \mathbb{R}^{2n}$ is the RVF given in (5), $\boldsymbol{\sigma}_k(\cdot)$, for $k = 1, 2$, is a column vector where each element is a linear saturation function (Definition 3). It is worth mentioning that each element of vector $\boldsymbol{\sigma}_k(\cdot)$ is bounded from above by M_k, with M_k as a constant satisfying $2M_1 < M_2$ and $\eta = 1[\mathrm{s}^{-1}]$ as a constant that allows us to add the position error with the velocity. In (Aranda-Bricaire and González-Sierra, 2023). it is proven that in the control law (10) in closed-loop with the system (1), the agents reach the desired geometric pattern and avoid collisions among them.

Remark 5. The control law presented in (10) differs from the one presented in (Aranda-Bricaire and González-Sierra, 2023). The main difference is that the RVFs are continuous in (10) while in (Aranda-Bricaire and González-Sierra, 2023) are discontinuous.

4. NUMERICAL SIMULATIONS

Two numerical simulations were carried out to compare the performance of both approaches. For the first numerical simulation, the simplest case of collision avoidance is considered, *i.e.*, the interchange of the position of two agents. On the other hand, for the second numerical simulation, the formation with collision avoidance for a group of nine agents is considered.

4.1 Two agents

For the first numerical simulation, two agents with a radius of 0.2[m] have to exchange their position. The initial positions of the agents are $\mathbf{z}_1(0) = [3\ 0]^{\top}$ and $\mathbf{z}_2(0) = [-3\ 0]^{\top}$, while the formation vectors are given by $\mathbf{c}_{21} = [-4\ 0]^{\top}$ and $\mathbf{c}_{12} = -\mathbf{c}_{21}$. The sensing distance is set to $D = 1$[m] and the safety distance is set to $d = 0.5$[m] while the function $\psi_{ij}(d_{ij})$ is defined as

$$\psi_{ij}(d_{ij}) = \frac{1}{1 + e^{a(d_{ij}-b)}}, \tag{11}$$

where $b = (D + d)/2$ and $a = 22$. Table 1 presents the parameters for the control strategies given in (6) and (10).

Table 1. Parameters for the first numerical simulation.

Parameter	**Backstepping (B)**	**Nested saturation (NS)**
ϵ	1	10
μ	1	-
λ	1	-
M_1	-	1.5
M_2	-	3.1

Figure 1 illustrates the trajectory in the plane comparison between the B and the NS approach. Note that both methodologies accomplish the formation control with collision avoidance; however, when using the B approach, the performance is smoother than when utilizing the NS approach. Furthermore, Fig. 2 depicts the distance between the agents, where it is worth pointing out that the distance between them is always greater than the safety distance.

The RMS values are calculated over a suitable receding-horizon time interval of finite length, *i.e.*

$$\mathbf{u}_{rms}(t) = \left(\frac{1}{\Delta T}\int_{t-\Delta T}^{t}\|\mathbf{u}(\tau)\|^2 d\tau\right)^{\frac{1}{2}},$$

$$\tilde{\mathbf{z}}_{rms}(t) = \left(\frac{1}{\Delta T}\int_{t-\Delta T}^{t}\|\tilde{\mathbf{z}}(\tau)\|^2 d\tau\right)^{\frac{1}{2}},$$

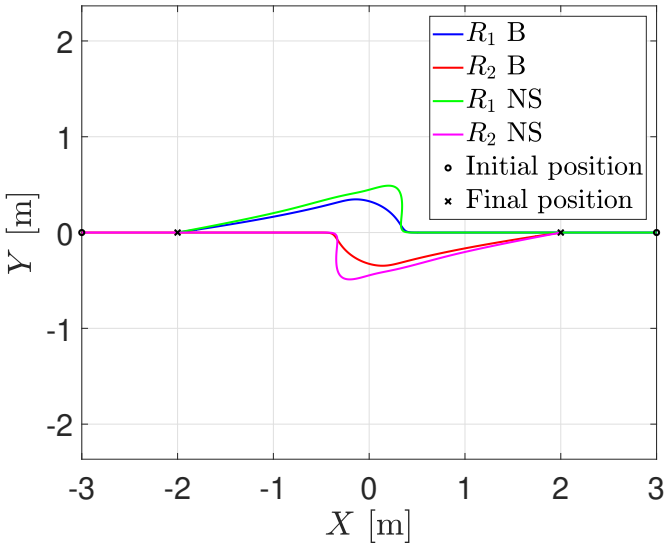

Fig. 1. Trajectory in the plane of the agents by using the B and NS approach.

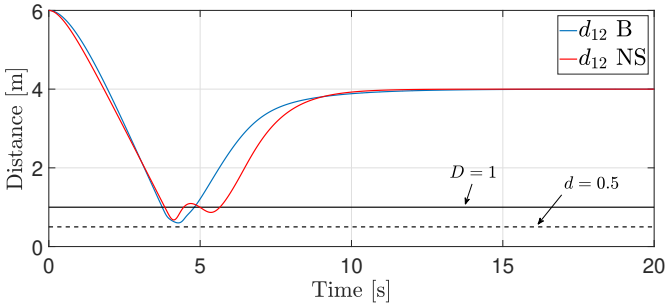

Fig. 2. Distance between the agents by using the B and NS approach.

where $\Delta T = 2$ is a time window width for the corresponding signal evaluation. Based on the above mentioned, the RMS control inputs and the RMS position errors are shown in Fig. 3(a) and 3(b), respectively. From Fig. 3(a), one can note that the control inputs have a similar performance. The NS has a greater peak, while the B presents two peaks of almost the same magnitude. Furthermore, the B converges to zero before the NS approach. This means that the agents reach their position faster with the B approach. On the other hand, from Fig. 3(b), it is evident that when using the NS, an over peak appears when the RVFs are turned on, while the performance is smoother for the B approach.

4.2 Nine agents

For this numerical simulation, nine agents have to reach the formation illustrated in Fig. 4. The initial positions are $\mathbf{z}_1(0) = [-15\ 0]^\top$, $\mathbf{z}_2(0) = [10\ 10]^\top$, $\mathbf{z}_3(0) = [-5\ 5]^\top$, $\mathbf{z}_4(0) = [-5\ -5]^\top$, $\mathbf{z}_5(0) = [5\ -5]^\top$, $\mathbf{z}_6(0) = [-10\ 10]^\top$, $\mathbf{z}_7(0) = [15\ 5]^\top$, $\mathbf{z}_8(0) = [15\ -10]^\top$ and $\mathbf{z}_9(0) = [5\ 5]^\top$, all with zero velocity. Furthermore, the formation vectors

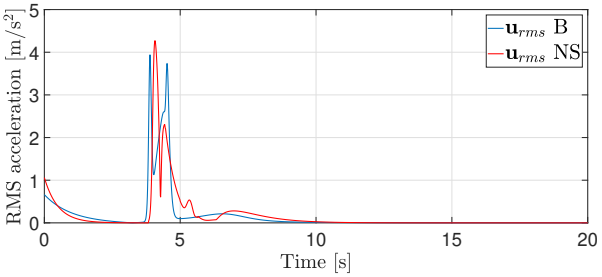

(a) RMS control inputs by using the B and NS approach.

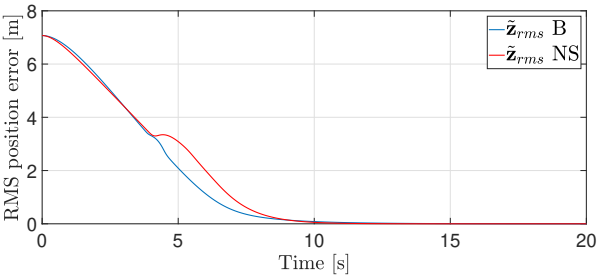

(b) RMS position error by using the B and NS approach.

Fig. 3. RMS control inputs and RMS position error.

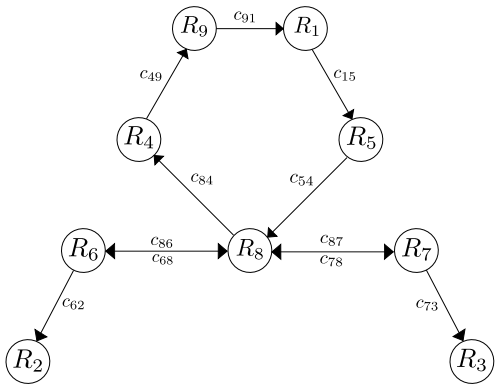

Fig. 4. Desired formation.

are given by $\mathbf{c}_{91} = \ell\,[3\ 0]^\top$, $\mathbf{c}_{62} = \ell\,[-1.5\ -3]^\top$, $\mathbf{c}_{73} = \ell\,[1.5\ -3]^\top$, $\mathbf{c}_{84} = \ell\,[-3\ 3]^\top$, $\mathbf{c}_{15} = \mathbf{c}_{73}$, $\mathbf{c}_{86} = \ell\,[-4.5\ 0]^\top$, $\mathbf{c}_{87} = -\mathbf{c}_{86}$, $\mathbf{c}_{58} = \ell\,[-3\ -3]^\top$, $\mathbf{c}_{78} = \mathbf{c}_{86}$, $c_{68} = -c_{86}$ and $\mathbf{c}_{49} = \ell\,[1.5\ 3]^\top$ which are parameterized by a scale factor $\ell = 1.3$[m]. The sensing distance is set to $D = 2.8$[m] and the safety distance is set to $d = 2$[m] while the function $\psi_{ij}(d_{ij})$ is defined as in (11) with $a = 10$. Table 2 presents the parameters for the control strategies given in (6) and (10).

Figure 5 depicts the trajectory in the plane of the nine agents by applying the B approach (Fig. 5(a)) and the NS methodology (Fig. 5(b)). Note that when using the NS, the agents move far away from their initial positions, while with the B, they are near their initial conditions. Nevertheless, with both approaches, the agents achieve the desired formation.

Table 2. Parameters for the second numerical simulation.

Parameter	Backstepping (B)	Nested saturation (NS)
ϵ	0.6	10
μ	1	-
λ	1	-
M_1	-	1.5
M_2	-	4

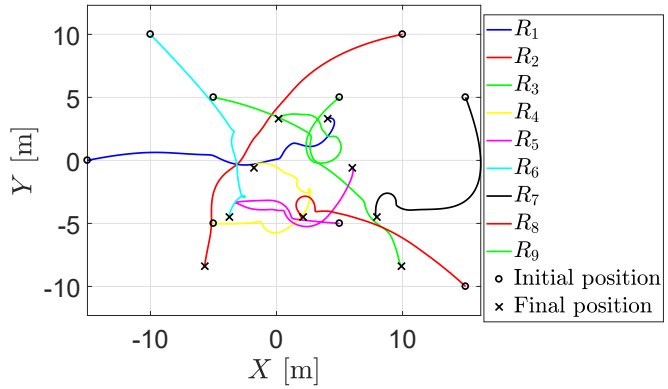

(a) Trajectory in the plane of the agents by using the B approach.

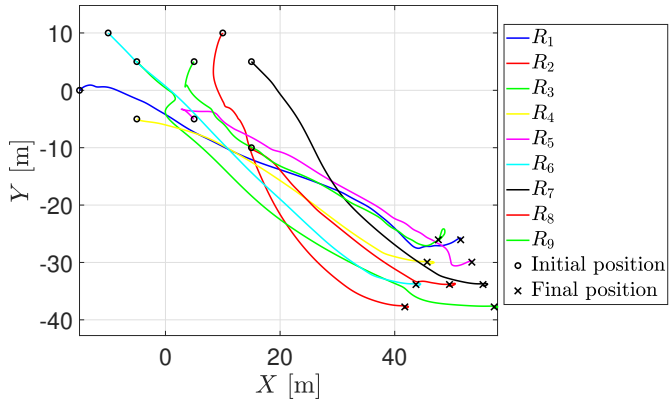

(b) Trajectory in the plane of the agents by using the NS approach.

Fig. 5. Trajectory in the plane of the agents by using the B and NS approach.

Figure 6 illustrates the distance between agents with both methodologies. It is worth mentioning that such distances are always greater than the safety distance; thus, there is no collision among the agents.

Finally, Fig. 7 presents the RMS control input (Fig. 7(a)) and the RMS position error (Fig. 7(b)). Specifically, from Fig. 7(a), it is clear that the NS approach uses more energy than the B methodology. Furthermore, from Fig. 7(b), one can note that the RMS position error is less than when using the B approach.

5. CONCLUSIONS AND OUTLOOKS

Two current control strategies for comparing the formation control with collision avoidance for a second-order

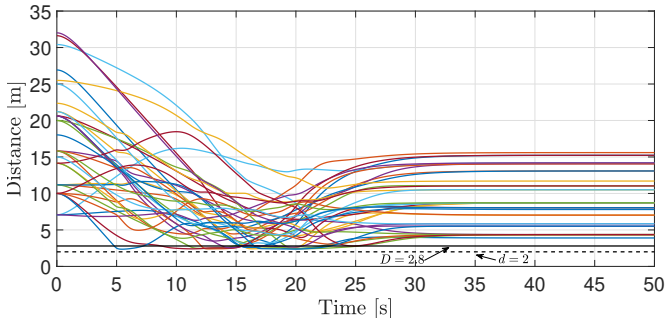

(a) Distance among the agents by using the B approach.

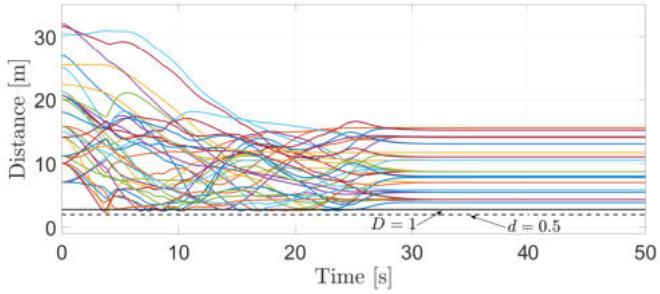

(b) Distance among the agents by using the NS approach.

Fig. 6. Distance among the agents utilizing the two approaches.

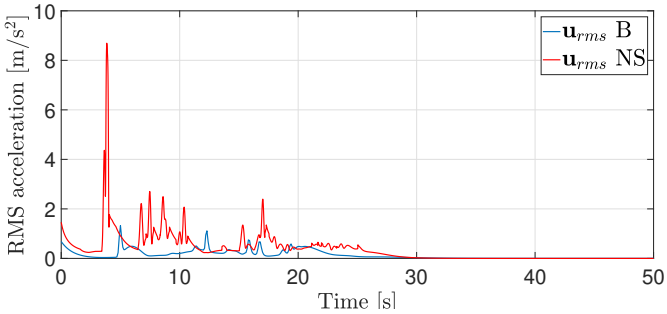

(a) RMS control inputs by using the B and NS approach.

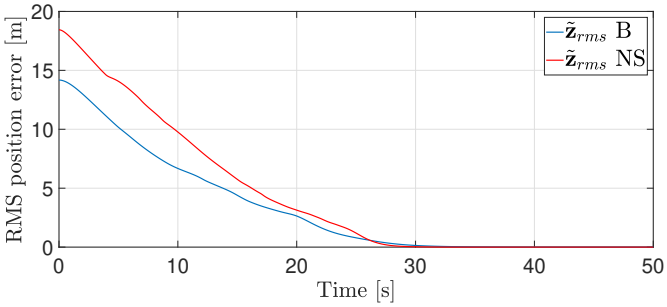

(b) RMS position error by using the B and NS approach.

Fig. 7. RMS control inputs and RMS position error.

multi-agent system are presented to evaluate their performance. For the first comparison, the interchange of the position of two agents is evaluated by calculating the RMS value of the control inputs and the position error. From the control inputs, the behavior is quite similar; however, the agents' motion is smoother with the B approach. The formation with collision avoidance for nine agents was tested for the second comparison. The RMS values show that the B approach requires less energy than the NS approach to reach the desired formation. Although both strategies accomplish the formation with collision avoidance, based on those mentioned earlier, the B methodology presents a better performance concerning the NS approach. On the other hand, it is worth mentioning that under the NS approach, the RVFs are applied only regarding relative positions between agents, while in the B approach, because of the design process, relative velocities are taken into account, which increases the complexity of the control law.

REFERENCES

Aranda-Bricaire, E. and González-Sierra, J. (2023). Formation with non-collision control strategies for second-order multi-agent systems. *Entropy*, 25(6). doi: 10.3390/e25060904.

Dang, A.D., La, H.M., Nguyen, T., and Horn, J. (2019). Formation control for autonomous robots with collision and obstacle avoidance using a rotational and repulsive force–based approach. *International Journal of Advanced Robotic Systems*, 16(3). doi: 10.1177/1729881419847897.

Draganjac, I., Miklić, D., Kovačić, Z., Vasiljević, G., and Bogdan, S. (2016). Decentralized control of multi-agv systems in autonomous warehousing applications. *IEEE Transactions on Automation Science and Engineering*, 13(4), 1433–1447. doi: 10.1109/TASE.2016.2603781.

Flores-Resendiz, J.F. and Aranda-Bricaire, E. (2020). A general solution to the formation control problem without collisions for first order multi-agent systems. *Robotica*, 38(6), 1123–1137. doi:10.1017/S0263574719001280.

Flores-Resendiz, J.F., Aranda-Bricaire, E., González-Sierra, J., and Santiaguillo-Salinas, J. (2015). Finite-time formation control without collisions for multiagent systems with communication graphs composed of cyclic paths. *Mathematical Problems in Engineering*, 1–17. doi:https://doi.org/10.1155/2015/948086.

Flores-Resendiz, J.F., Avilés, D., and Aranda-Bricaire, E. (2023). Formation control for second-order multi-agent systems with collision avoidance. *Machines*, 11(2). doi:10.3390/machines11020208. URL `https://www.mdpi.com/2075-1702/11/2/208`.

Godsil, C. and Royle, G. (2001). Algebraic graph theory. *Graduate Texts in Mathematics, Springer, New York, NY, USA*, 207.

Guanghua, W., Deyi, L., Wenyan, G., and Peng, J. (2013). Study on formation control of multi-robot systems. In *2013 Third International Conference on Intelligent System Design and Engineering Applications*, 1335–1339. doi:10.1109/ISDEA.2012.316.

Hernandez-Martinez, E. and Aranda-Bricaire, E. (2013). Collision avoidance in formation control using discontinuous vector fields. *IFAC Proceedings Volumes*, 46(23), 797–802. doi: https://doi.org/10.3182/20130904-3-FR-2041.00175.

Hernández-Martínez, E.G. and Aranda-Bricaire, E. (2011). Convergence and collision avoidance in formation control: A survey of the artificial potential functions approach. In F. Alkhateeb, E.A. Maghayreh, and I.A. Doush (eds.), *Multi-Agent Systems*, chapter 6, 103–126. IntechOpen. doi:10.5772/14142.

Huang, S., Teo, R.S.H., and Tan, K.K. (2019). Collision avoidance of multi unmanned aerial vehicles: A review. *Annual Reviews in Control*, 48, 147–164. doi: https://doi.org/10.1016/j.arcontrol.2019.10.001.

Khatib, O. (1985). Real-time obstacle avoidance for manipulators and mobile robots. In *Proceedings. 1985 IEEE International Conference on Robotics and Automation*, volume 2, 500–505. doi: 10.1109/ROBOT.1985.1087247.

Liu, J., Zhao, M., and Qiao, L. (2022). Adaptive barrier lyapunov function-based obstacle avoidance control for an autonomous underwater vehicle with multiple static and moving obstacles. *Ocean Engineering*, 243, 110303. doi:10.1016/j.oceaneng.2021.110303.

Madridano, A., Al-Kaff, A., Martín, D., and de la Escalera, A. (2021). Trajectory planning for multi-robot systems: Methods and applications. *Expert Systems with Applications*, 173, 114660. doi: https://doi.org/10.1016/j.eswa.2021.114660.

Park, B.S. and Yoo, S.J. (2021). Connectivity-maintaining and collision-avoiding performance function approach for robust leader–follower formation control of multiple uncertain underactuated surface vessels. *Automatica*, 127(C). doi: 10.1016/j.automatica.2021.109501.

Parra-Marín, A., Aranda-Bricaire, E., and González-Sierra, J. (2023). Collision avoidance for second-order mobile robots. *Memorias del Congreso Nacional de Control Automático, Tuxtla Gutiérrez, Chiapas, México*, 469–474.

Ren, W. and Beard, R.W. (2008). Distributed consensus in multi-vehicle cooperative control:theory and applications. *Communications and Control Engineering Series, Springer, London, UK*.

Teel, A.R. (1992). Global stabilization and restricted tracking for multiple integrators with bounded controls. *Systems & Control Letters*, 18, 165–171.

Yan, L. and Ma, B. (2019). Practical formation tracking control of multiple unicycle robots. *IEEE Access*, 7, 113417–113426. doi:10.1109/ACCESS.2019.2931750.

Yasin, J.N., Mohamed, S.A.S., Haghbayan, M.H., Heikkonen, J., Tenhunen, H., and Plosila, J. (2020). Unmanned aerial vehicles (uavs): Collision avoidance systems and approaches. *IEEE Access*, 8, 105139–105155. doi:10.1109/ACCESS.2020.3000064.